2010

Model Of Sprite Luminous Trail Caused By Increasing Streamer Current

Ningyu Liu

Model of sprite luminous trail caused by increasing streamer current

Ningyu Liu[1]

Received 16 December 2009; accepted 8 January 2010; published 25 February 2010.

[1] This study investigates a possible physical mechanism responsible for the occurrence of the luminous trail of sprite streamers, which is also known as "afterglow." According to streamer modeling results, when sprite streamers propagate with expansion, acceleration and brightening, the total current flowing through the streamer body also increases. The increasing current results in the rise of the electric field in the streamer channel far behind the streamer head, which leads to effective production of N_2 excited states by electron impact excitation and then the glowing trail. **Citation:** Liu, N. Y. (2010), Model of sprite luminous trail caused by increasing streamer current, *Geophys. Res. Lett.*, *37*, L04102, doi:10.1029/2009GL042214.

1. Introduction

[2] High speed video observations with submillisecond resolution provide detailed time dynamics of sprite streamer development [*Cummer et al.*, 2006; *McHarg et al.*, 2007; *Stenbaek-Nielsen et al.*, 2007; *Stenbaek-Nielsen and McHarg*, 2008; *Li and Cummer*, 2009]. Observations demonstrate that typical initial sprite streamers accelerate, expand during their propagation, and their emission is enhanced in the region of streamer heads, which is then followed by a dark channel. The analysis of the high speed videos further reveals that sprite streamer heads are brightening during their propagation [*Stenbaek-Nielsen et al.*, 2007; *Stenbaek-Nielsen and McHarg*, 2008]. All those observed features are consistent with the streamer theory of air discharges at sprite altitudes [e.g., *Pasko et al.*, 1998; *Raizer et al.*, 1998; *Liu and Pasko*, 2004, 2005; *Pasko*, 2007; *Liu et al.*, 2009a, 2009b]. Further, the observations also show that the dark channel well behind the descending streamer head brightens over time in the vicinity of the region of its initiation [*McHarg et al.*, 2007; *Stenbaek-Nielsen et al.*, 2007]. This trail is also referred to as "afterglow."

[3] Recent work discusses the origin of the streamer luminous trail [e.g., *Sentman et al.*, 2008; *Gordillo-Vázquez*, 2008; *Stenbaek-Nielsen and McHarg*, 2008; *Sentman and Stenbaek-Nielsen*, 2009]. The physical mechanisms, which could lead to the production of the luminous trail, include the production of the excited species leading to sprite emission by the energy transfer from N_2 and O_2 metastable electronic states, energy pooling between low energy metastable states and between those states with vibrationally excited N_2 ground states [e.g., *Morrill et al.*, 1998; *Bucsela et al.*, 2003; *Kanmae et al.*, 2007; *Pasko*, 2007; *Sentman et al.*, 2008; *Sentman and Stenbaek-Nielsen*, 2009]. However, numerical modeling results of streamers also show the presence of a luminous trail, although the above-mentioned chemical processes are not taken into account [e.g., *Liu et al.*, 2009a, 2009b].

[4] The purpose of this paper is to analyze the origin of the luminous trail of the model streamer. Our study shows the total current (sum of conduction and displacement currents) flowing along the streamer increases as the streamer accelerates, expands and brightens. The increasing current requires the electric field in the streamer trail to rise, which leads to effective production of N_2 excited states by electron impact excitation in this region and the formation of the luminous trail.

2. Problem Formulation

[5] The nitrogen afterglow phenomena have been studied for many years in laboratory experiments. They are found in the downstream region of electrical discharges maintained by flowing N_2 gas mixtures. As the gas has passed the active plasma discharge region, the afterglow is normally considered as a secondary chemiluminescent process where electron impact excitation plays a negligible role. A discussion about the possible mechanisms is presented by *Sentman et al.* [2008]. Those mechanisms include the production of $N_2(B^3\Pi_g)$, which lead to the first positive band system of N_2 emission ($1PN_2$), by the energy pooling of vibrationally excited N_2 ground states $N_2(X^1\Sigma_g^+,\ 5 \le v \le 14)$ with $N_2(A^3\Sigma_u^+)$, and by the energy pooling between $N_2(A^3\Sigma_u^+)$ states. The metastable states $N_2(A^3\Sigma_u^+)$ can also react with $O_2(a^1\Delta_g)$ to produce $N_2(B^3\Pi_g)$. Another possible chemical process for the production of $N_2(B^3\Pi_g)$ is the deactivation of $N_2(a'^1\Sigma_u^-)$ by N_2 molecules. However, *Sentman and Stenbaek-Nielsen* [2009] demonstrate the energy pooling between $N_2(A^3\Sigma_u^+)$ states and those states with $O_2(a^1\Delta_g)$ results in negligible contribution in production of $N_2(B^3\Pi_g)$ comparing to the electron impact excitation, when the streamer channel field is greater than $0.25E_k$ (E_k is the breakdown threshold field), which is likely to be the case according to streamer modeling results. Under the same field condition, the energy pooling of vibrationally excited N_2 ground states with $N_2(A^3\Sigma_u^+)$ is also negligible according to the following estimate using the kinetic modeling results from *Sentman et al.* [2008]. The reaction rate constant for the energy pooling process between $N_2(X^1\Sigma_g^+,\ 5 \le v \le 14)$ and $N_2(A^3\Sigma_u^+)$ is about 2×10^{-17} m^3/s, and the densities of $N_2(X^1\Sigma_g^+,\ v = 1)$ and $N_2(A^3\Sigma_u^+)$ are 5×10^{13} 1/m^3 and 1×10^{13} 1/m^3, respectively. Because the electron impact excitation rates of higher vibrational levels are much smaller, the total density of $N_2(X^1\Sigma_g^+,\ v = 5\text{–}14)$ is 10 times the density of $N_2(X^1\Sigma_g^+,\ v = 1)$ at the most. The resulting pro-

[1]Department of Physics and Space Sciences, Florida Institute of Technology, Melbourne, Florida, USA.

0094-8276/10/2009GL042214$05.00

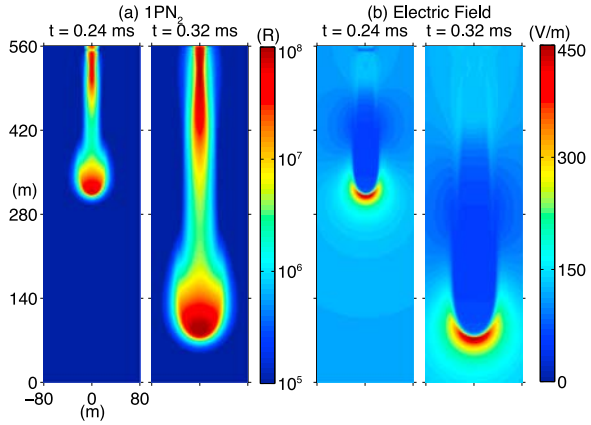

Figure 1. (a) Emission intensity of $1PN_2$ in Rayleighs and (b) cross-sectional view of electric field for a model streamer at two instants of time: 0.24 and 0.32 ms. The model positive streamer propagates downward from 75 km altitude in an electric field of 35 N/N_0 kV/cm.

duction rate of $N_2(B^3\Pi_g)$ is 1×10^{11} $1/m^3/s$ maximum. This value is much smaller than the production rate of 2×10^{13} $1/m^3/s$ by electron impact excitation using a channel electron density of 10^{12} $1/m^3$ (typical value for a streamer at 70 km altitude) and a channel field of $0.25E_k$.

[6] To investigate how the luminous trail appears in the streamer model where the above-mentioned chemiluminescent processes are not included [e.g., *Liu and Pasko*, 2004; *Liu et al.*, 2009a], we consider a modeling case of a positive streamer developing in a uniform ambient field of 35 N/N_0 kV/cm at 75 km altitude, where N and N_0 are the air density at 75 km and 0 km altitudes, respectively. The direction of the ambient field is set as downward. The streamer initiates and then propagates downward. A neutral plasma cloud with a spherically symmetric Gaussian spatial distribution is introduced at the start of the simulation for the initiation of the streamer. The plasma cloud is centered at the axis of symmetry and 6 m below the top boundary, and its characteristic scale and peak density are 6 m and 1.2×10^{11} $1/m^3$, respectively. The size of computational domain is 560×80 m^2, which corresponds to a discharge gap of 1.86×0.27 cm^2 at atmospheric pressure.

3. Results and Discussion

[7] Figure 1a shows the modeling results of the emission intensity of $1PN_2$ in Rayleighs at two instants of time: 0.24 and 0.32 ms. The emission is highly enhanced in the streamer head, a relatively dark streamer channel immediately follows the bright streamer head, and then a bright luminous trail comes after the dark channel. The trail extends toward the direction of streamer propagation and its size increases as the streamer propagates. The cross-sectional views of the electric field for those two times are shown by Figure 1b. The luminosity of the streamer coincides with the high field region of the streamer. The field is peaked at the streamer head, where the emission intensity is strongest. A relatively strong field region is present just below the top boundary and its size grows with time. This region is coincident with the luminous trail found in Figure 1a.

[8] The electron density and the field along the symmetry axis at several moments of time are illustrated by Figure 2. The breakdown field E_k at 75 km altitude is also plotted as a reference field. It can be clearly seen that the electron density in the region well behind the head rises during the streamer propagation. At t = 0.32 ms, the peak density in this region is about 3–4 times greater than the density just behind the streamer head. In the same region, the field increases then levels off to a value larger than E_k. Such a strong field causes the increase of the electron density in this region. The small drop in the electron density around the vertical dashed line for the t = 0.32 ms curve is caused by the loss of electrons by two body electron attachment process. As the field here grows from the small magnitude in the channel to E_k, the electron attachment dominates over electron impact ionization leading to the reduction of electron density.

[9] To investigate the physical mechanism responsible for the rise of the electric field in the region corresponding to the luminous trail, we consider the total current flowing through the streamer body. This current can be evaluated using Shockley-Ramo (SR) theorem [*Shockley*, 1938; *Ramo*, 1939]. It states that the external current I flowing into an individual conductor of a system of conductors due to moving space charge (its velocity $\vec{v}$ is specified) inside a volume V bounded by the conductors can be calculated by $I = \frac{1}{\phi_a}\int_V \rho\vec{v}\cdot\vec{E}_L d\tau$, where $d\tau$ is elementary volume, and ρ is the space charge density. The electric field $\vec{E}_L$ is calculated under the condition that the conductor under investigation has a potential of ϕ_a while the rest conductors are grounded and the space charge is ignored. Its physical meaning is the conductor needs to supply the power to

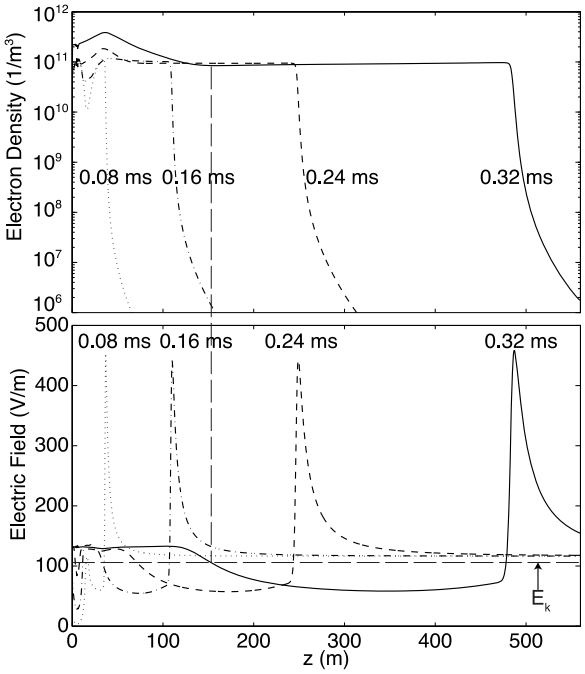

Figure 2. Profiles of (top) electron density and (bottom) electric field of the model streamer along the symmetry axis at several instants of time: 0.08, 0.16, 0.24 and 0.32 ms. The z axis points in the direction of streamer propagation and the streamer initiates at 75 km altitude. The vertical dashed line aligns the region of density drop at the crossing of $E = E_k$.

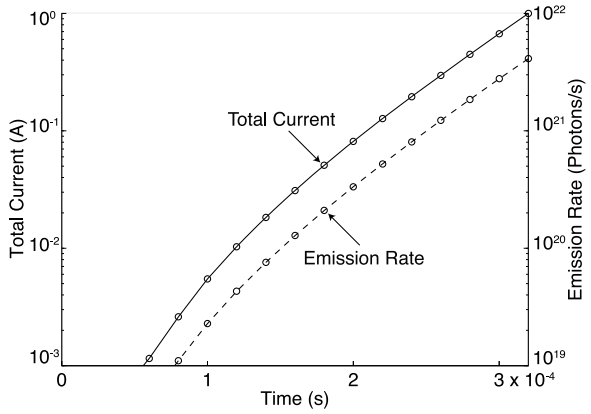

Figure 3. The time variations of the total current and the total emission rate of the model streamer. The total current is labeled on the left while the emission rate labeled on the right. Circles are data points calculated from the modeling results.

accelerate the charge by its own field only. A detailed derivation of this formula using Green's theorem and conservation of energy is given by *Jen* [1941]. For the streamer problem considered here, the top boundary is assumed to be a perfect conductor and the SR theorem is used to calculate the external current flowing into it, which then continuously flows as a sum of conduction current and displacement current through the discharge region. Ions are motionless because of the short timescale of the problem so that $I = -\frac{2\pi e}{\phi_a}\int_0^d\int_0^R n_e\vec{v}_e\cdot\vec{E}_L r dr dz$ after taking into account cylindrical symmetry, where e is elementary charge, d and R are the length and radius of the discharge gap, and, n_e and $\vec{v}_e$ are the density and velocity of electrons. It should be noted n_e and $\vec{v}_e$ are taken from the streamer simulation results and the above formula calculates the instantaneous current induced by the moving electrons in the streamer discharge.

[10] The calculated total current flowing into the top boundary is shown on log scale by Figure 3. The current carried by the streamer increases very fast and after about t = 0.16 ms the data points are approximately on a straight line. The emission rate from the whole streamer is also plotted on Figure 3, which is known to grow exponentially with time [*Stenbaek-Nielsen et al.*, 2007; *Liu et al.*, 2009a]. The growth rates for the two quantities are the same because the two curves are parallel to each other.

[11] We further consider the distribution of the conduction current along the streamer body. The conduction current is calculated as $I_c(z) = -2\pi e\int_0^R(n_e\vec{v}_e)\cdot\hat{z}rdr$. The result is shown by Figure 4 for t = 0.32 ms along with the total current and the field profiles. The conduction current is peaked in the streamer head and negligible in front of the streamer head. In the regions corresponding to the streamer head and the channel right behind the head the conduction current is larger than the total current. The field in those regions must decrease to give a negative displacement current, which means that the strong electric field in the region around the current streamer head and channel, shown by Figure 1, will be reduced as the streamer moves forward. The conduction current in the trail is smaller than the total current, so the field increase is necessary to produce a positive displacement current. The positive gradient of the conduction current in the streamer channel along the z direction implies that charge is transferred from here to the region ahead of the streamer to form a new streamer head as the streamer continues to develop. Figure 4 also shows that the field in the trail starts to increase at the crossing of the total current and the conduction current. Hence, according to Figures 3 and 4, the electric field in the streamer trail rises during the streamer development because an increasing total current flows through the streamer body while the conduction current in the trail is smaller than this total current. Observational and modeling studies have established that sprite streamers expand and brighten during their initial stage of development. As the electron density and the electric field in the moving streamer head stay relatively constant, the expansion of the streamer head must be accompanied by the increase of the conduction current. However, because the transverse size of the channel is unvarying after its formation, the only means to raise the current in the trail far behind the head is to increase the field. It is also expected that this trail starts to appear at the origin of the sprite streamer and then extends toward the direction of the propagation as long as the streamer keeps on expanding and brightening.

[12] We conclude by discussing whether the assumption of a perfect conductor for the top boundary of the streamer simulation affects the validity of the conclusions drawn here. In reality, the lower ionosphere is neither homogenous nor perfectly conducting. However, large scale modeling of sprites has demonstrated that a sharp increase of electron density exists in the altitude range of 80–85 km prior to initiation of sprite streamers [e.g., *Pasko et al.*, 1997; *Hu et al.*, 2007]. The electron density reaches a value of $>10^8$ 1/m^3 at the top of this region. The corresponding Maxwellian relaxation time is several microseconds, which is much shorter than the timescale of the streamer propagation considered in the present work. *Hu et al.* [2007, Figure 4] show that the lightning field quickly relaxes at 86 km altitude while persists at 81 km. Sprite streamers are very likely to initiate at the bottom of this sharp transition region and the perfect conductor assumption seems reasonable. In fact, a recent study reports the modeling results of sprite streamers

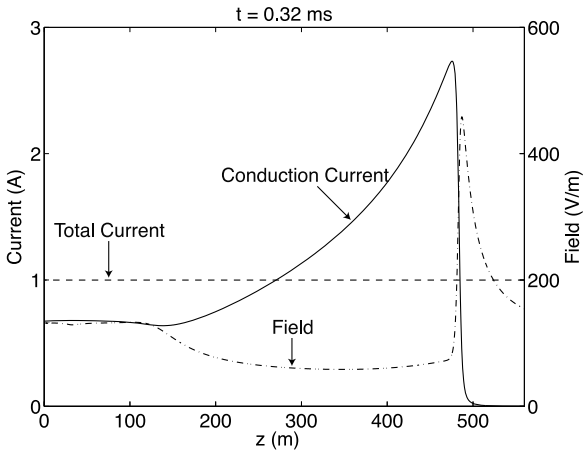

Figure 4. The conduction current along the model streamer at t = 0.32 ms. The z axis points in the direction of streamer propagation. The field profile on the symmetry axis gives the location of different streamer regions. The dashed line represents the total current flowing across the streamer.

initiating from the lower ionosphere boundary [*Luque and Ebert*, 2009], where the rise of the field after the streamer head is also present, although a luminous trail is not clearly shown, which is possibly due to averaging of the emission in both time and space domains comparing to the present work.

[13] **Acknowledgments.** This research was supported in part by NSF grant ATM 0838867 to Florida Institute of Technology.

References

Bucsela, E., J. Morrill, M. Heavner, C. Siefring, S. Berg, D. Hampton, D. Moudry, E. Wescott, and D. Sentman (2003), $N_2(B^3\Pi_g)$ and $N_2^+(A^2\Pi_u)$ vibrational distributions observed in sprites, *J. Atmos. Sol. Terr. Phys.*, *65*, 583–590.

Cummer, S. A., N. Jaugey, J. Li, W. A. Lyons, T. E. Nelson, and E. A. Gerken (2006), Submillisecond imaging of sprite development and structure, *Geophys. Res. Lett.*, *33*, L04104, doi:10.1029/2005GL024969.

Gordillo-Vázquez, F. J. (2008), Air plasma kinetics under the influence of sprites, *J. Phys. D Appl. Phys.*, *41*, 234016, doi:10.1088/0022-3727/41/23/234016.

Hu, W., S. A. Cummer, and W. A. Lyons (2007), Testing sprite initiation theory using lightning measurements and modeled electromagnetic fields, *J. Geophys. Res.*, *112*, D13115, doi:10.1029/2006JD007939.

Jen, C. K. (1941), On the induced current and energy balance in electronics, *Proc. IRE*, *29*, 345–349.

Kanmae, T., H. C. Stenbaek-Nielsen, and M. G. McHarg (2007), Altitude resolved sprite spectra with 3 ms temporal resolution, *Geophys. Res. Lett.*, *34*, L07810, doi:10.1029/2006GL028608.

Li, J., and S. A. Cummer (2009), Measurement of sprite streamer acceleration and deceleration, *Geophys. Res. Lett.*, *36*, L10812, doi:10.1029/2009GL037581.

Liu, N. Y., and V. P. Pasko (2004), Effects of photoionization on propagation and branching of positive and negative streamers in sprites, *J. Geophys. Res.*, *109*, A04301, doi:10.1029/2003JA010064.

Liu, N. Y., and V. P. Pasko (2005), Molecular nitrogen LBH band system far-UV emissions of sprite streamers, *Geophys. Res. Lett.*, *32*, L05104, doi:10.1029/2004GL022001.

Liu, N. Y., V. P. Pasko, K. Adams, H. C. Stenbaek-Nielsen, and M. G. McHarg (2009a), Comparison of acceleration, expansion, and brightness of sprite streamers obtained from modeling and high-speed video observations, *J. Geophys. Res.*, *114*, A00E03, doi:10.1029/2008JA013720.

Liu, N. Y., V. P. Pasko, H. U. Frey, S. B. Mende, H.-T. Su, A. B. Chen, R.-R. Hsu, and L.-C. Lee (2009b), Assessment of sprite initiating electric fields and quenching altitude of $a^1\Pi_g$ state of N_2 using sprite streamer modeling and ISUAL spectrophotometric measurements, *J. Geophys. Res.*, *114*, A00E02, doi:10.1029/2008JA013735.

Luque, A., and U. Ebert (2009), Emergence of sprite streamers from screening-ionization waves in the lower ionosphere, *Nat. Geosci.*, *2*, 757–760, doi:10.1038/NGEO662.

McHarg, M. G., H. C. Stenbaek-Nielsen, and T. Kammae (2007), Observations of streamer formation in sprites, *Geophys. Res. Lett.*, *34*, L06804, doi:10.1029/2006GL027854.

Morrill, J. S., E. J. Bucsela, V. P. Pasko, S. L. Berg, W. M. Benesch, E. M. Wescott, and M. J. Heavner (1998), Time resolved N_2 triplet state vibrational populations and emissions associated with red sprites, *J. Atmos. Sol. Terr. Phys.*, *60*, 811–829.

Pasko, V. P. (2007), Red sprite discharges in the atmosphere at high altitude: The molecular physics and the similarity with laboratory discharges, *Plasma Sources Sci. Technol.*, *16*, S13–S29, doi:10.1088/0963-0252/16/1/S02.

Pasko, V. P., U. S. Inan, T. F. Bell, and Y. N. Taranenko (1997), Sprites produced by quasi-electrostatic heating and ionization in the lower ionosphere, *J. Geophys. Res.*, *102*, 4529–4561, doi:10.1029/96JA03528.

Pasko, V. P., U. S. Inan, and T. F. Bell (1998), Spatial structure of sprites, *Geophys. Res. Lett.*, *25*, 2123–2126.

Raizer, Y. P., G. M. Milikh, M. N. Shneider, and S. V. Novakovski (1998), Long streamers in the upper atmosphere above thundercloud, *J. Phys. D Appl. Phys.*, *31*, 3255–3264.

Ramo, S. (1939), Currents induced by electron motion, *Proc. IRE*, *27*, 584–585.

Sentman, D. D., and H. C. Stenbaek-Nielsen (2009), Chemical effects of weak electric fields in the trailing columns of sprite streamers, *Plasma Sources Sci. Technol.*, *18*, 034012, doi:10.1088/0963-0252/18/3/034012.

Sentman, D. D., H. C. Stenbaek-Nielsen, M. G. McHarg, and J. S. Morrill (2008), Plasma chemistry of sprite streamers, *J. Geophys. Res.*, *113*, D11112, doi:10.1029/2007JD008941.

Shockley, W. (1938), Currents to conductors induced by a moving point charge, *J. Appl. Phys.*, *9*, 635–636.

Stenbaek-Nielsen, H. C., and M. G. McHarg (2008), High time-resolution sprite imaging: Observations and implications, *J. Phys. D Appl. Phys.*, *41*, 234009, doi:10.1088/0022-3727/41/23/234009.

Stenbaek-Nielsen, H. C., M. G. McHarg, T. Kanmae, and D. D. Sentman (2007), Observed emission rates in sprite streamer heads, *Geophys. Res. Lett.*, *34*, L11105, doi:10.1029/2007GL029881.

N. Y. Liu, Department of Physics and Space Sciences, Florida Institute of Technology, 150 W. University Blvd., Melbourne, FL 32901, USA. (nliu@fit.edu)